

Sl. No.	<p style="text-align: center;"><b>IIT Ropar</b>  <b>List of Recent Publications with Abstract</b>  <b>Coverage: January, 2022</b></p>
1.	<p><a href="#">A BER-conscious Synthesis of Switched-beam Antenna to Maximize Reliable Coverage in WSN Applications</a>  S Kumar, S Jain, A Sharma - IEEE Sensors Journal, 2022</p> <p><b>Abstract:</b> A BER-conscious synthesis of switched multi-beam multi-sector access point (AP) antenna is proposed to enhance reliable communication coverage for WSN applications. The sector-based design of multi-beam AP antenna is necessary for a densely deployed WSN to achieve high system capacity with 360° azimuth coverage. However, the neighboring sectors cause high co-channel interference resulting in a low signal to interference (SIR) ratio and hence degrades the communication link quality. This leads to frequent packet re-transmissions resulting in increased energy consumption at the power deficient sensor nodes. The proposed BER-conscious array synthesis scheme incorporates projected power and SIR limits within the antenna design process to maximize the effective coverage area with acceptable BER. The optimized coverage with reliable communication implies energy saving at the sensor nodes. Based on the proposed process of coverage optimization, a multi-sector AP antenna is analytically synthesized. A prototype is fabricated, and the analytically obtained coverage results are verified through experiments. The maximum radial range of 2 - 13 m with 360° communication coverage is achieved. Moreover, high port isolation of 45.95 dB between adjacent sectors enables the generation of multiple simultaneous beams in the communication region resulting in high system capacity. The achieved performance indicates that the synthesized switched multi-beam multi-sector antenna using the proposed scheme is a good candidate for AP in WSN applications.</p>
2.	<p><a href="#">A Blockchain and Machine Learning based IoT Framework to Improve Contract Farming</a>  S Saxena, S Khare, S Pal - IEEE Globecom Workshops, 2021</p> <p><b>Abstract:</b> Farming sector forms a major part of the Indian economy. It makes a contribution of about 14% to the Gross Domestic Product (GDP) of the country. Despite holding such an essential place in the Indian economy, this sector has seen very little technology penetration. The farmers have been plagued with poor economic conditions. Contract Farming is seen as a viable solution for this problem, as it involves tie-up of corporate firms with farmers, which comes with its many benefits. In this work, we focus on facilitating Contract Farming so that both the firm and the farmer can reap benefits. Using Blockchain, IoT and Machine Learning techniques, we make it feasible for a corporate firm to supervise a farming operation according to specific needs while safeguarding the farmer from unfair exploitation.</p>
3.	<p><a href="#">A continuous–discontinuous localizing gradient damage framework for failure analysis of quasi-brittle materials</a>  A Negi, S Kumar - Computer Methods in Applied Mechanics and Engineering, 2022</p> <p><b>Abstract:</b> This article presents a continuous–discontinuous approach that provides a discontinuous character to the quasi-brittle fracture process, modeled in a continuous setting through a micromorphic stress-based localizing gradient damage framework. The discontinuous framework is developed by enhancing the problem fields using discontinuous interpolations in the critically damaged regions exploiting local partition of unity via the eXtended Finite Element Method (XFEM). The proposed approach incorporates an improved spatial nonlocal diffusive</p>

	<p>behavior in the continuous bulk through an additional microforce balance equation to ensure an improved prediction of the initial phase of the loading process. Level sets are computed to track the discontinuity within the finite element mesh, predicted via evolving micromorphic equivalent strain. Here, the proposed continuous–discontinuous approach combines the advantages of the gradient damage method and the XFEM while exhibiting improved convergence using low-order finite elements during numerical simulations. The enhanced numerical kinematics of the proposed approach successfully eliminates damage spreading during the final failure stages and provides an accurate description of a true discontinuity without using cohesive zone modeling. Various representative structural examples of benchmark tests involving varying loading conditions are investigated to demonstrate the accuracy and robustness of the proposed approach to provide qualitative and quantitative accurate numerical predictions.</p>
4.	<p><a href="#">A fabric tensor based small strain constitutive law for the elastoplastic behavior of snow</a>  AK Singh, PK Srivastava, N Kumar, P Mahajan - <i>Mechanics of Materials</i>, 2022</p> <p><b>Abstract:</b> The mechanical behavior of snow depends on its density and microstructure. The anisotropy in the microstructure is expressed in terms of fabric tensor that leads to an anisotropic stress-strain relation. Lately, fabric-based relations have successfully estimated the elastic properties of snow. Motivated by this, we propose a fabric-based macroscopic elasto-plastic constitutive law for snow, which can be used to study avalanche initiation. Mean Intercept Length tensor used as a measure of material fabric is determined by X-ray tomography. Fabric tensor and density-dependent yield surface with a provision for isotropic hardening/softening are used in this process. Beyond the initial yield, the yield function grows till the strength of the snow is reached and then softens. Since snow exhibits tension and compression behavior asymmetry, a piece-wise quadratic yield function is used. Stress-strain curves needed for determining the equation of the hardening/softening law and other parameters of the proposed macroscopic constitutive law are obtained through micro-Finite Element (<math>\mu</math>-FE) simulations. The macroscopic constitutive law has been implemented as a user subroutine in a FE code and can predict the snow's multi-axial behavior.</p>
5.	<p><a href="#">A novel NiVP/Pi based flexible sensor for direct electrochemical ultrasensitive detection of cholesterol</a>  N Thakur, D Mandal, TC Nagaiah - <i>Chemical Communications</i>, 2022</p> <p><b>Abstract:</b> A novel non-enzymatic electrochemical sensor was constructed to deal with the problems related to serious coronary heart diseases for highly selective and ultrasensitive detection of cholesterol. The NiVP/Pi based sensor exhibits ultra-high sensitivity of <math>5510.18 \mu\text{A} \mu\text{M}^{-1} \text{cm}^{-2}</math> and other at <math>36.8 \mu\text{A} \mu\text{M}^{-1} \text{cm}^{-2}</math> from 1 nM to 10 <math>\mu\text{M}</math> and 100 <math>\mu\text{M}</math> to 10 mM range, respectively and ultra-low detection limit of 1 aM, along with superior selectivity towards various interferents like ascorbic acid, glucose and uric acid. Besides, novel NiVP/Pi based flexible sensor coated over Whatman filter paper was developed and displayed superior sensitivity, even with human blood serum sample at physiological pH in physiologically range.</p>
6.	<p><a href="#">A Planar Distributed Multicoil Antenna to Generate 3-D Ellipsoidally Polarized H-field for Angular Misalignment Tolerant WPT System</a>  VK Srivastava, A Sharma, A Bharadwaj - <i>IEEE Transactions on Antennas and Propagation</i>, 2022</p> <p><b>Abstract:</b> This paper presents 3-D polarized magnetic-field forming using a planar multicoil</p>

	<p>transmitter antenna for WPT applications. Three orthogonal H-field components resulting in optimized 3-D ellipsoidal polarization are generated to mitigate the angular misalignment problem by the proposed antenna. The analytical optimization of the 3-D polarized H-field is presented, and its effect on induced voltage in the receiver coil is investigated. To achieve unconstrained induced voltage in the receiver independent of its angular movement, an optimized planar multicoil design is proposed for a maximum S21 between the transmitter and the receiver coil antennas. Unlike the 3-D transmitter designs available in the literature, the proposed antenna is a 2-D planar PCB design, therefore, represents a cost-effective solution and is suitable for various practical WPT applications. The analytical results of the design are verified experimentally. The result proves that the proposed antenna is able to completely mitigate the angular misalignment problem, which represents a potential planar antenna solution for orientation-insensitive wireless power transfer applications.</p>
7.	<p><a href="#">A review on morphology, nanostructure, chemical composition, and number concentration of diesel particulate emissions</a>  S Rana, MR Saxena, RK Maurya - Environmental Science and Pollution Research, 2022</p> <p><b>Abstract:</b> Particulate matter (PM) emitted from compression ignition (CI) engines (diesel engines) has a detrimental effect on human health and the environment. The physical and chemical characteristics of PM emitted from CI-engines are influenced by engine operating conditions and fuel properties. The morphology, nanostructure, and chemical composition of PM affect its toxicity and interaction with the environment. From automotive industry perspective, these parameters influence the design of diesel particulate filters. This study presents a review of the physical and chemical characteristics of particulate emissions from the CI-engine. The present study commences with a brief description about the composition of PM emitted from CI-engine and the PM formation mechanism in CI-engine. Later on, the detailed review of PM's physical and chemical characteristics and the effect of engine operating parameters and alternative fuels on the particle number concentration, morphology, nano-structure, and oxidative reactivity of PM is presented. Online and offline methods of diesel particulate characterization and emerging chemical characterization techniques such as X-ray photoelectron spectroscopy and X-ray absorption fine structure (EXAFS) are also discussed briefly. Correlation between physical and chemical properties, and oxidative reactivity of PM is also discussed. It was found that engine operating parameters affect the physical and chemical properties of PM. Use of alternative fuels changes the diesel particulate morphology, nanostructure, and chemical composition which enhances the oxidative reactivity of PM.</p>
8.	<p><a href="#">A Seismic Sensor based Human Activity Recognition Framework using Deep Learning</a>  P Choudhary, N Goel, M Saini - 17th IEEE International Conference on Advanced Video and Signal Based Surveillance, 2021</p> <p><b>Abstract:</b> Activity recognition has gained attention due to the rapid development of microelectromechanical sensors. Numerous human-centric applications in healthcare, security, and smart environments can benefit from an efficient human activity recognition system. In this paper, we demonstrate the use of a seismic sensor for human activity recognition. Traditionally, researchers have relied on handcrafted features to identify the target activity, but these features may be inefficient in complex and noisy environments. The proposed framework employs an autoencoder to map the activity into a compact representative descriptor. Further, an Artificial Neural Network (ANN) classifier is trained on the extracted descriptors. We compare the</p>

	<p>proposed framework with multiple machine learning classifiers and a state-of-the-art framework on different evaluation metrics. On 5-fold cross-validation, the proposed approach outperforms the state-of-the-art in terms of precision and recall by an average of 10.68 and 23.36%, respectively. We also collected a dataset to assess the efficacy of the proposed seismic sensor-based activity recognition. The dataset is collected in a variety of challenging environments, such as variable grass length, soil moisture content, and the passing of unwanted vehicles nearby.</p>
9.	<p><a href="#">A Switchable Multi-Coil Antenna With Booster Coil to Improve Coverage in WPT Systems</a>  A Bharadwaj, VK Srivastava, A Sharma, CC Reddy - IEEE Transactions on Antennas and Propagation, 2021</p> <p><b>Abstract:</b> In this paper, a planar distributed multi-coil transmitter antenna is presented for wireless power transfer (WPT) applications. The proposed antenna is optimized to mitigate lateral misalignment problem and configured to operate in two different modes. The antenna switched to the normal mode excites a chief coil to form a concentrated H-field within the perfectly aligned receiver area. Encircling the chief coil, a set of booster coils is incorporated in the design which is switched on in enhanced mode to stretch the H-field uniformity whenever the receiver is misaligned. As a result, the proposed design evolves into a switchable planar distributed multi-coil (SPDMC) antenna. Using a field forming technique based on a minimum mean square error algorithm, dimensional parameters of the proposed antenna are optimized. The proposed antenna improves stability in the power transfer efficiency which is verified by measuring the S21 parameter. The S21 stability achieved in the Rx working area is 98×98 mm<sup>2</sup> which corresponds to a 255% improvement over an existing design of same dimension in the literature. The proposed SPDMC antenna is proved to be highly insensitive to lateral misalignment and a good antenna candidate for various short and medium-range WPT applications.</p>
10.	<p><a href="#">Adaptive and Progressive Multispectral Image Demosaicking</a>  M Gupta, V Rathi, P Goyal - IEEE Transactions on Computational Imaging, 2022</p> <p><b>Abstract:</b> Common consumer RGB cameras use a single image sensor to capture RGB color images with a color filter array (CFA) placed in front of the image sensor. This system captures particularly one color sample (R, G, or B) at each pixel location. This captured raw image is called a CFA image. The CFA demosaicking is used then to construct the complete color image. A similar approach of working with a single image sensor and extension of CFA to multispectral filter array (MSFA) enables us to develop a low-cost multispectral camera with the help of MSFA demosaicking. However, due to many spectral bands and their very sparse sampling, extending CFA demosaicking to MSFA demosaicking is not easy. This paper proposes an adaptive and progressive MSFA demosaicking method for various MSFA patterns for 5 to 15 bands multispectral images. Binary tree-based MSFA patterns are used to create MSFA images, and these MSFA patterns can be designed for any N-band MSFA image. The spectral bands are arranged specifically so that the middle band has the highest probability of appearance (PoA) in the MSFA pattern. The middle band is interpolated first using PoA based progressive adaptive interpolation, and the modified bilinear spectral difference method is used to estimate all other spectral bands with the interpolated middle bands help. Experimental results and comparative analysis on two different datasets reveal that our proposed MSFA demosaicking method outperforms the existing generic MSFA demosaicking methods in terms of computational time and various image quality metrics considered.</p>

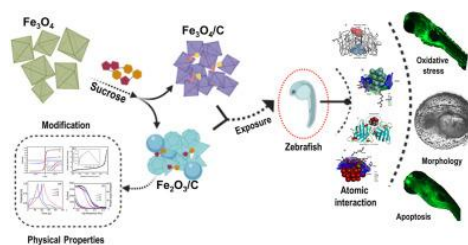
[Altered electrochemical properties of iron oxide nanoparticles by carbon enhance molecular biocompatibility through discrepant atomic interaction](#)

SK Verma, A Thirumurugan, PK Panda, P Patel...R. Ahuja - *Materials Today Bio*, 2021

11.

**Abstract:** Recent advancement in nanotechnology seeks exploration of new techniques for improvement in the molecular, chemical, and biological properties of nanoparticles. In this study, carbon modification of octahedral-shaped magnetic nanoparticles (MNPs) was done using two-step chemical processes with sucrose as a carbon source for improvement in their electrochemical application and higher molecular biocompatibility. X-ray diffraction analysis and electron microscopy confirmed the alteration in single-phase octahedral morphology and carbon attachment in  $\text{Fe}_3\text{O}_4$  structure. The magnetization saturation and BET surface area for  $\text{Fe}_3\text{O}_4$ ,  $\text{Fe}_3\text{O}_4/\text{C}$ , and  $\alpha\text{-Fe}_2\text{O}_3/\text{C}$  were measured as 90, 86, and 27 emu/g and 16, 56, and 89  $\text{m}^2/\text{g}$  with an average pore size less than 7 nm. Cyclic voltammogram and galvanostatic charge/discharge studies showed the highest specific capacitance of carbon-modified  $\text{Fe}_3\text{O}_4$  and  $\alpha\text{-Fe}_2\text{O}_3$  as 213 F/g and 192 F/g. The *in vivo* biological effect of altered physicochemical properties of  $\text{Fe}_3\text{O}_4$  and  $\alpha\text{-Fe}_2\text{O}_3$  was assessed at the cellular and molecular level with embryonic zebrafish. Mechanistic *in vivo* toxicity analysis showed a reduction in oxidative stress in carbon-modified  $\alpha\text{-Fe}_2\text{O}_3$  exposed zebrafish embryos compared to  $\text{Fe}_3\text{O}_4$  due to despaired influential atomic interaction with sod1 protein along with significant less morphological abnormalities and apoptosis. The study provided insight into improving the characteristic of MNPs for electrochemical application and higher biological biocompatibility.

**Graphical Abstract:**



[An Optimized Machine Learning Model Accurately Predicts In-Hospital Outcomes at Admission to a Cardiac Unit](#)

SC Bollepalli, AK Sahani, N Aslam, B Mohan... - *Diagnostics*, 2022

12.

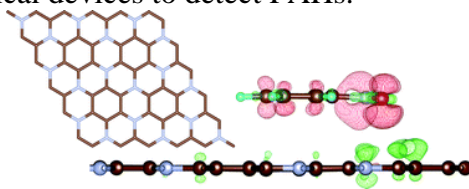
**Abstract:** Risk stratification at the time of hospital admission is of paramount significance in triaging the patients and providing timely care. In the present study, we aim at predicting multiple clinical outcomes using the data recorded during admission to a cardiac care unit via an optimized machine learning method. This study involves a total of 11,498 patients admitted to a cardiac care unit over two years. Patient demographics, admission type (emergency or outpatient), patient history, lab tests, and comorbidities were used to predict various outcomes. We employed a fully connected neural network architecture and optimized the models for various subsets of input features. Using 10-fold cross-validation, our optimized machine learning model predicted mortality with a mean area under the receiver operating characteristic curve (AUC) of 0.967 (95% confidence interval (CI): 0.963–0.972), heart failure AUC of 0.838 (CI: 0.825–0.851), ST-segment elevation myocardial infarction AUC of 0.832 (CI: 0.821–0.842), pulmonary embolism AUC of 0.802 (CI: 0.764–0.84), and estimated the duration of stay (DOS)



	<p>with a mean absolute error of 2.543 days (CI: 2.499–2.586) of data with a mean and median DOS of 6.35 and 5.0 days, respectively. Further, we objectively quantified the importance of each feature and its correlation with the clinical assessment of the corresponding outcome. The proposed method accurately predicts various cardiac outcomes and can be used as a clinical decision support system to provide timely care and optimize hospital resources.</p>
13.	<p><a href="#"><u>Analysis of Frequency Response of Transformer with Inter-Turn Short Circuit Fault due to Transients</u></a>  B Das, S Dhayalan, EV Reddy, BS Thind, CC Reddy - IEEE 5th International Conference on Condition Assessment Techniques in Electrical Systems, 2021</p> <p><b>Abstract:</b> Transformer insulation is mainly designed based on lightning and switching impulse voltage. The standard lightning impulse waveform is 1.2/50 <math>\mu</math>sec. Very Fast Transient Overvoltage (VFTO) has a smaller rise time of about 4-100 nanoseconds, followed by some oscillations of about 1 to 50 MHz. The chopped impulse can be classified into two types, if chopping occurs before peak value is reached, the impulse is chopped on front, if it is chopped on the tail, called tail chopped. The chopped impulse and VFTO, if present in the power system network, causes severe degradation of transformer insulation, which may lead to failure or premature breakdown. In this paper, the VFTO and tail time chopped signals are examined on the transformer for inter-turn fault. These test signals are injected into a transformer winding under no-load condition. The frequency response is scrutinized for the healthy and faulty scenario of the transformer in terms of statistical parameters such as Absolute Average Difference (D.A.B.S.), Minimum Maximum Ratio (M.M. absolute), and Comparative Standard Deviation (C.S.D.). These statistical parameters are calculated for a different number of shorted turns on the LV winding of the transformer. Based on these statistical parameters, the variation in the frequency response plots is examined for the healthy and faulty conditions of the transformer.</p>
14.	<p><a href="#"><u>Analysis of Low and High Temperature Heat Release in Dual-Fuel RCCI Engine and its Relationship with Particle Emissions</u></a>  MR Saxena, S Rana, RK Maurya - Journal of Energy Resources Technology, 2022</p> <p><b>Abstract:</b> This study presents the influence of low-temperature heat release (LTHR) and high-temperature heat release (HTHR) on the combustion and particle number characteristics of the RCCI engine. The study investigates the relationship between the amount of LTHR, HTHR, and particle number emission characteristics. In this study, gasoline and methanol are used as low reactivity fuel (LRF), and diesel is used as a high reactivity fuel (HRF). The LRF is injected into the intake manifold using a port-fuel injection (PFI) strategy, and HRF is directly injected into the cylinder using a direct injection strategy. A particle sizer is used to measure particle emission in size ranging from 5 to 1000 nm. Firstly, the LTHR and HTHR are analyzed for different diesel injection timing (SOI) for RCCI operation. Later, the variation of particle emissions with LTHR and HTHR is characterized. Additionally, empirical correlations are developed to understand the relation between the LTHR and HTHR with particle emission. Two-staged auto-ignition of charge has been observed in RCCI combustion. Results depict that LTHR varies with diesel injection timing and the phasing of HTHR depends on the amount and location of LTHR. Results also showed that HTHR and LTHR significantly influence the formation of particle number concentration in RCCI combustion. The developed empirical correlation depicts a good correlation between diesel SOI and the ratio of HTHR to LTHR to estimate total particle number</p>

	concentration.
15.	<p><a href="#">Approximation Algorithm and Hardness Results for Defensive Domination in Graphs</a>  MA Henning, A Pandey, V Tripathi - International Conference on Combinatorial Optimization and Applications, 2021</p> <p><b>Abstract:</b> In a graph <math>G=(V,E)</math>, a non-empty set <math>A</math> of <math>k</math> distinct vertices, is called a <math>k</math>-attack on <math>G</math>. The vertices in the set <math>A</math> is considered to be under attack. A set <math>D \subseteq V</math> can defend or counter the attack <math>A</math> on <math>G</math> if there exists a one to one function <math>f:A \rightarrow D</math>, such that either <math>f(u)=u</math> or there is an edge between <math>u</math> and it's image <math>f(u)</math>, in <math>G</math>. A set <math>D</math> is called a <math>k</math>-defensive dominating set, if it defends against any <math>k</math>-attack on <math>G</math>. Given a graph <math>G=(V,E)</math>, the minimum <math>k</math>-defensive domination problem requires us to compute a minimum cardinality <math>k</math>-defensive dominating set of <math>G</math>. When <math>k</math> is not fixed, it is co-NP-hard to decide if <math>D \subseteq V</math> is a <math>k</math>-defensive dominating set. However, when <math>k</math> is fixed, the decision version of the problem is NP-complete for general graphs. On the positive side, the problem can be solved in linear time when restricted to paths, cycles, co-chain graphs and threshold graphs for any <math>k</math>. In this paper, we mainly focus on the problem when <math>k &gt; 0</math> is fixed. We prove that the decision version of the problem remains NP-complete for bipartite graphs, this answers a question asked by Ekim et al. (Discrete Math. 343 (2) (2020)). We give lower and upper bound on the approximation ratio for the problem. Further, we show that the minimum <math>k</math>-defensive domination problem is APX-complete for bounded degree graphs. On the positive side, we show that the problem is efficiently solvable for complete bipartite graphs for any <math>k &gt; 0</math>.</p>
16.	<p><a href="#">Assessing the Impact of COVID-19 on Interactions Among Stock, Gold and Oil Prices in India</a>  P Mukherjee, S Bardhan - Revisiting the Indian Financial Sector, Part of the India Studies in Business and Economics book series, 2022</p> <p><b>Abstract:</b> This chapter explores the relationship between stock and commodity prices in the derivatives market, in the Indian context. In order to estimate the long-term relationship, ARDL model is employed on daily data during the period of 2017–2020. The chapter also incorporates the impact of market disruptions on the relationship, following the recent COVID-19 pandemic. The findings indicate that the stock returns and the prices of crude oil and gold are closely related. Interestingly, findings also suggest that the pandemic has altered the relationship. For example, there was no evidence of cointegration among the stock, gold and crude oil prices during the pre-COVID period. However, post-pandemic, evidence of cointegrating relationships exists. Apart from that, some interesting insights from the short-run relationship between the two markets include a mutual influence on each other in the pre-pandemic period; e.g. stock returns are determined by past values of gold and oil price, whereas stock market returns affect volatility in oil price. However, during the COVID period, volatility of gold prices, in addition to crude oil prices, seems to be driving the stock returns.</p>
17.	<p><a href="#">Binding and optical characteristics of polycyclic aromatic hydrocarbons and their nitroderivatives adsorbed on the C3N monolayer</a>  S Deshpande, M Deshpande, T Hussain, R Ahuja - New Journal of Chemistry, 2022</p> <p><b>Abstract:</b> Carbon–nitrogen based two dimensional frameworks have attracted significant attention due to their great potential for environmental applications. Among the <math>g-C_xN_y</math> family, the C3N monolayer (ML) is one of the promising candidates, which exhibits semiconducting behavior. The structural, electronic and optical properties of the polycyclic aromatic</p>

hydrocarbons (PAHs) and their nitroderivatives adsorbed on the C<sub>3</sub>N ML have been investigated using first principles calculations. We chose six representative molecules from the PAH family, benzene (B), anthracene (A), and benzo[a]pyrene (BaP), and their nitroderivatives, nitrobenzene (NB), 9-nitroanthracene (NA), and 6-nitro-benzo[a]pyrene (NBaP). These molecules are severely affecting human beings and aquatic systems. The optimal adsorption orientation of these molecules on the C<sub>3</sub>N ML is determined and the adsorption energies ( $E_{\text{ads}}$ ) are calculated. The  $E_{\text{ads}}$  of these PAH molecules with C<sub>3</sub>N ML are found to be higher than that of graphene. The PAH molecules with the nitro group show higher  $E_{\text{ads}}$  as compared to that of molecules without the nitro group. Further, we have checked the implicit water solvation effect on the adsorption behavior of PAHs on the C<sub>3</sub>N ML. In a water solvent,  $E_{\text{ads}}$  further increases. The energy gap of the C<sub>3</sub>N ML is sensitive to the adsorption of these nitroderivatives of the PAH molecules, which implies the possibility of its use as a sensor. We have noticed an increase in the calculated work function upon the adsorption of PAH molecules which further explains the affinity of the C<sub>3</sub>N ML towards these molecules. The static dielectric constant  $\epsilon_1(0)$  and the refractive index ( $n(0)$ ) of the pristine C<sub>3</sub>N ML are 4.24 and 2.06, respectively. Adsorption of B, A and BaP molecules on C<sub>3</sub>N does not have a significant impact on the values of  $\epsilon_1(0)$  and  $n(0)$ . But adsorption of their nitroderivatives shows a notable increase in the values of  $\epsilon_1(0)$  and  $n(0)$ . We believe that our results could trigger further theoretical and experimental work towards constructing highly sensitive nanosensors and optical devices to detect PAHs.



[Conscientiousness moderates the relationship between neuroticism and health-risk behaviors among adolescents](#)

P Singh - Scandinavian Journal of Psychology, 2022

18.

**Abstract:** Health-Risk-Behaviors (HRBs) are considered significant antecedent conditions of adolescents' poor health and mortality. Prevention of any adverse health outcome requires an in-depth understanding of the risk and protective factors associated with its development and maintenance. Among other potential causal pathways, the “neuroticism- HRBs-adverse health” link has been supported in previous studies. Trait neuroticism has been associated with poor health and HRBs, but several moderators were also observed, which might transform neuroticism into a desirable phenomenon, that is, healthy neuroticism, that leads to better health. Conscientiousness is one such potential moderator; however, the moderating effect of conscientiousness in the neuroticism-HRBs link has not been explored extensively among adolescents, especially in India; therefore, no conclusive evidence is available. Thus, the present study was planned to explore the moderating effect of conscientiousness in the relationship between neuroticism and HRBs among adolescents. The study was conducted in India and its cross-sectional sample, procured through a multi-stage stratified random sampling, consists of 648 (364 males) adolescents (Mage = 16.08). Participants provided relevant information on standardized questionnaires. Moderated regression analysis was applied to test the stated hypotheses. Individuals high on neuroticism and low on conscientiousness reported more indulgence in health-risk behaviors than individuals high on both neuroticism and conscientiousness. It indicates that a higher level of conscientiousness may reduce the negative



	<p>impact that neuroticism has on HRBs. The findings imply that the assessment of conscientiousness and strategies to increase the same should be part of interventional programs to achieve adolescents' wellbeing.</p>
19.	<p><a href="#">Design and Performance Benchmarking of Dual Gate Flexible Bilayer Graphene FETs</a> S Pathania, P Gupta, R Kumar, S Kumar - IEEE Bombay Section Signature Conference, 2021</p> <p><b>Abstract:</b> It has reached a period when the search beyond silicon for utilizing it in a transistor has increased genuine significance. Graphene is described as a crystalline allotrope of carbon with two-dimensional properties arranged in the hexagonal lattice form. It's one of the uses in designing field-effect transistors (FET) such as graphene field-effect transistors. It is explored for the future of flexible electronics devices applications due to the promising graphene attributes. There is some parameter that decides the performance such as speed, uniformity, and reliability of the GFET. One can use graphene field-effect transistors (GFET) to design analog and digital applications for future technology nodes. In this paper, we present a mathematical model of flexible bilayer dual-gated graphene FETs and implement it in a Verilog–A.</p>
20.	<p><a href="#">Development of Modular Library for Rapid Prototyping of Planar Hybrid Linkages using Computer Aided Design: Design of a modular library using CAD for prototyping of different planer hybrid linkages via additive manufacturing techniques</a> S Ranjan, S Gupta, E Singla - Advances in Robotics - 5th International Conference of The Robotics Society, 2021</p> <p><b>Abstract:</b> The paper targets to develop a modular library for prototyping planar hybrid linkages using additive manufacturing, while suggesting an optimized selection of printing conditions, layering direction, and clearances. A safe range for pure tensile load has been estimated using FEM simulation to confirm usability in prototyping. Three modules have been designed to produce active, passive, and joint locking functionalities in the revolute joints and the fourth connectivity module helps to achieve the connectivity in between revolute joints of different linkages. It has been shown by developing the prototype for two different complex planer hybrid manipulators as examples, that these modules work as tools for the designer to design a customized manipulator. CAD modelling has been used for preparing a complete manipulator structure which, using AM, can be given the physical form.</p> <p>In the design and manufacturing of robotic manipulators, incorporating modular libraries makes the design customizable as well as makes the process easier. With this approach, the user follows a drag and drop approach to customize a design using an already available set of modular components fulfilling different purposes. Further work will demonstrate the technique by preparing models some randomly selected linkages based upon the designed modules.</p>
21.	<p><a href="#">Effects of low and high viscous product on Kelvin–Helmholtz instability triggered by A+ B→ C type reaction</a> SN Maharana, M Mishra - Physics of Fluids, 2022</p> <p><b>Abstract:</b> The dynamics of the Kelvin–Helmholtz (K–H) instability triggered by a non-linear second order <math>A+B\rightarrow C</math> type reaction is analyzed through direct numerical simulations. This paper aims to understand the chemo-hydrodynamic K–H instability when the chemical reaction decreases or increases the viscosity gradient at the reactive interface. Thus, we consider the viscosity of the obtained product C is to be different from both the iso-viscous reactants A and B. It is observed that for both the cases of less and more-viscous product C, K–H roll-ups occur at</p>

	<p>the reactive interface and hence various flow features are compared for both of these scenarios. Moreover, depending on the product's viscosity, the flow-directed K–H roll-ups occur either at A–C interface or C–B interface. Strikingly the number of K–H roll-ups at the reactive interface is more when the product is less viscous and full vortex completion of K–H roll-ups is noticed. It is demonstrated that even for a significantly large Damköhler number (high rate of reaction), the K–H roll-ups may not occur at the reactive front. Thus, a favorable log-mobility ratio (<math>M_c</math>) having a greater magnitude than the critical log-mobility ratio (<math>M_c^{crit}</math>) is required to trigger the K–H instability within a desirable time for both the cases of <math>M_c &lt; 0</math> and <math>M_c &gt; 0</math>. Moreover, asymmetric onset dynamics are encountered with respect to <math>M_c = 0</math> axis.</p>
22.	<p><a href="#">Efficacy of carbon nanotubes and polydimethylsiloxane interlayer in augmenting the impact strength of glass fiber/epoxy composites</a>  N Yadav, J Bhinder, PK Agnihotri - Proceedings of the Institution of Mechanical Engineers, Part L: Journal of Materials: Design and Applications, 2022</p> <p><b>Abstract:</b> An experimental investigation is carried out to explore the possibility of carbon nanotubes addition and incorporation of polydimethylsiloxane soft interlayer in improving the impact strength and energy-absorbing capability of conventional glass fiber-reinforced plastics. To this end, deformation behavior of glass fiber-reinforced plastics, carbon nanotube-modified glass fiber-reinforced plastics, and glass fiber-reinforced plastics-polydimethylsiloxane sandwich coupons under high strain rate loading are compared using the split-Hopkinson pressure bar testing technique. While neat epoxy is used to process conventional glass fiber-reinforced plastics, the carbon nanotubes-modified glass fiber-reinforced plastics samples are fabricated using 0.5 wt. % carbon nanotube-modified epoxy. The split-Hopkinson pressure bar testing reveals that the addition of carbon nanotubes improves the peak stress and energy-absorbing capacity of the epoxy matrix. The improved impact response of carbon nanotube-modified epoxy translates into enhanced peak stress and energy-absorbing capability of carbon nanotubes-modified glass fiber-reinforced plastics in comparison to conventional glass fiber-reinforced plastics under impact loading. The microscopy analysis of failed composite samples reveals that while glass fiber-reinforced plastics primarily fails at the fiber/epoxy interface, the failure initiates in the epoxy matrix in carbon nanotubes-modified glass fiber-reinforced plastics samples. The impact testing of sandwich samples shows that the insertion of neat and 0.05 wt. % carbon nanotube-modified polydimethylsiloxane interlayer helps to distribute the impact load in a wider domain and thus delays the failure of glass fiber-reinforced plastics sandwich coupons. Moreover, the carbon nanotube-modified polydimethylsiloxane interlayer is better suited to increase the damage resistance and energy-absorbing ability of glass fiber-reinforced plastics. The present study provides a feasible strategy to enhance the failure strength and energy-absorbing capacity of conventional composites using carbon nanotube-modified epoxy and polydimethylsiloxane-based interlayer.</p>
23.	<p><a href="#">Electrical Characterization of Carbon Fiber Reinforced Polymer Composites</a>  H Gupta, PK Agnihotri, S Basu... - IEEE Electrical Insulation Conference, 2021</p> <p><b>Abstract:</b> Carbon fiber reinforced polymers (CFRP) composites are a promising alternative to metals for aircraft structures. The applicability of CFRP composites to electromagnetic shielding and immunity to lightning strikes depends largely on their electrical conductivity. In this work CFRP laminate were prepared by using pre-preg carbon fiber (fiber pre-impregnated with epoxy resin), and their electrical conductivity and shielding effectiveness (SE) were measured. Four-</p>

	<p>point probe method is used to measure electrical conductivity of CFRP as this method avoids errors due to contact resistance. SE is a measure of how effectively a material blocks an electromagnetic field and is measured in X-band (8.2-12.4 GHz) frequency using a Vector Network Analyzer (VNA). Composite slabs made with ten plies of prepregs, aligned unidirectionally seen to provide better electromagnetic attenuation (&gt;90%).</p>
24.	<p><a href="#">Emotion regulation difficulties mediate the relationship between neuroticism and health-risk behaviours in adolescents</a>  P Singh - <i>The Journal of Psychology</i>, 2021</p> <p><b>Abstract:</b> Health-Risk-Behaviors (HRBs) are significant antecedent conditions of adolescents' poor health and mortality. Prevention of avoidable adverse health outcomes requires an in-depth understanding of the factors associated with such outcomes. Among other possible pathways, the 'Neuroticism- HRBs-adverse health' link has been supported in previous studies. However, more extensive exploration of this link is required to identify the underlying modifiable risk factors. In the present study, one such factor, namely, emotion regulation difficulties, was explored to see its mediating effect in the relationship between neuroticism and HRBs—the first two constructs of the mentioned link. In this quantitative study, a total of 759 adolescents belonging to the Indian state of Punjab (Males= 402; M(age)=16.08) provided relevant information on a set of standardized questionnaires. Mediation analysis supported the major hypothesis of the present study. The results suggest that emotion regulation difficulty may be a significant mediator in the neuroticism-HRBs link. One's difficulty in regulating emotions might be an underlying mechanism through which high neuroticism increases the probability of indulging in HRBs, resulting in adverse health outcomes. The study implies that the assessment of emotion regulation difficulties should be included in interventional programs aimed at achieving adolescents' wellbeing, and early intervention may avoid progression toward adverse health outcomes in adulthood.</p>
25.	<p><a href="#">Emotion regulation difficulties, perceived parenting and personality as predictors of health-risk behaviours among adolescents</a>  P Singh - <i>Current Psychology</i>, 2022</p> <p><b>Abstract:</b> Health-Risk Behaviours (HRBs) are significant antecedent conditions of adverse health outcomes among adolescents, and their prevention requires an in-depth understanding of associated factors. Like any other behaviour, HRBs may be an outcome of a complex interplay between personal and situational factors that determines our responses. Among other factors, emotional tendencies, specific behavioural patterns, and psychosocial environment may be the significant factors working at different hierarchical positions within a system and guiding human behaviours, including HRBs. Previous studies have explored the role of these specific factors in developing and maintaining HRBs, but mainly among the adult population, and no conclusive results could be observed regarding their contribution to HRBs in adolescents. The present study explored the predictability of adolescents' engagement in HRBs with regard to three representations of the mentioned factors, i.e., emotion regulation difficulties, perceived parenting practices and personality traits. A total of 723 (Males = 440) adolescents (M<sub>age</sub> = 16.05, SD = 1.1) provided relevant information on the standardized questionnaires. Structural equation modelling was applied to test the stated hypotheses. Analysis revealed that the adolescents who reported more difficulty regulating one's emotions, perceived parenting practice as maladaptive, scored high on neuroticism and low on conscientiousness, showed more engagement in HRBs than their</p>

	<p>counterparts. Further, the findings indicated that emotion regulation difficulties and perceived parenting practices are stronger predictors of HRBs than personality traits. Interventional programs targeting HRBs among adolescents should address specific facets of emotional dysregulation and sensitise parents about their role in moderating adolescents' HRBs.</p>
26.	<p><a href="#">Estimation of Electric Field and Temperature in HVDC Cables Under Different Environmental Conditions</a>  S Dhayalan, A Das, P Johri, CC Reddy - IEEE 16th International Conference on Industrial and Information Systems, 2021</p> <p><b>Abstract:</b> With the advent of transmitting power through the HVDC cable, polymeric insulation is gradually taking place over the mass impregnated and oil-impregnated paper because of its various benefits. Polymeric HVDC cables have excellent electrical and thermal properties, especially in design stress which is comparatively low with mass and oil-impregnated insulation. However, having these benefits and large studies, the study about the effect of transients such as polarity reversal for different load and ambient conditions are still not well addressed. To have a successful long-term life of the cable, better understanding the effect of the change in environmental temperature, especially for the soil, is needed. During transients, the insulation undergoes high electro-thermal stress, and with the inclusion of the change in soil temperature can even be more catastrophic. In this paper, the actual electro-thermal model of the cable was considered for simulation along with the non-linear DC conductivity was incorporated in this model for enhancing the exact performance of the cable. The transient condition was performed according to Cigré standard TB 496. The simulation was performed to obtain the change in electric field and temperature over this insulation in a wide range of environmental temperatures. The peak electric field has been analyzed.</p>
27.	<p><a href="#">Experiment and Simulation of Leakage Current in HVDC Cable under Different Electro-Thermal Stresses</a>  S Dhayalan, B Das, P Johri, CC Reddy - IEEE 5th International Conference on Condition Assessment Techniques in Electrical Systems, 2021</p> <p><b>Abstract:</b> In the recent decades, HVDC XLPE cables have been in use for long distance transmission of power. A good insulator must have very low conductivity, low losses and high thermal stability. It is believed that, impurities, multiple voids, moisture and other contamination in the insulation may lead to increase in leakage current which causes losses in insulation, eventually leading to degradation or failure of insulation. Under high electric and thermal stresses, during transients such as switching, high load and sudden change in loads may lead to a faster rate of degradation of the insulation. So, it's important to measure insulation leakage current to identify the status of insulation. In this paper, the authors have experimentally measured the leakage current of an actual XLPE cable under different electro-thermal stresses. The leakage current has also been simulated under similar stresses using interdependent distributed electrical and thermal circuit models. The nonlinearly varying DC conductivity of the insulation, characterized experimentally, has been incorporated in the simulation. The multi-factor dependency has been implemented in the circuit simulation. Using simulation model, the leakage current can be estimated for varying electric and thermal fields.</p>
28.	<p><a href="#">Fermionic Bell violation in the presence of background electromagnetic fields in the cosmological de Sitter spacetime</a>  MS Ali, S Bhattacharya, S Chakraborty, S Kaushal – Physical Review D, 2021</p>

	<p><b>Abstract:</b> The violation of the Bell inequality for Dirac fermions is investigated in the cosmological de Sitter spacetime, in the presence of background electromagnetic fields of constant strengths. The orthonormal Dirac mode functions are obtained and the relevant in-out squeezed state expansion in terms of the Bogoliubov coefficients are found. We focus on two scenarios here: strong electric field and heavy mass limits (with respect to the Hubble constant). Using the squeezed state expansion, we then demonstrate the Bell violations for the vacuum and some maximally entangled initial states. Even though a background magnetic field alone cannot create particles, in the presence of background electric field and or spacetime curvature, it can affect the particle creation rate. Thus, our chief aim here is to investigate the role of the background magnetic field strength in the Bell violation. Qualitative differences in this regard for different maximally entangled initial states are shown. Further extension of these results to the so-called <math>\alpha</math> vacua are also discussed.</p>
29.	<p><a href="#">First-principles calculations to investigate electronic structure and optical properties of 2D MgCl<sub>2</sub> monolayer</a>  HR Mahida, A Patel, D Singh ...R Ahuja - Superlattices and Microstructures, 2022</p> <p><b>Abstract:</b> In the present work, we have concentrated on the structural, electronic, and optical properties of single-layer phase MgCl<sub>2</sub>. When bulk MgCl<sub>2</sub> reduces to monolayer form, then it exhibited indirect to direct bandgap transformation. The result indicates that the monolayer MgCl<sub>2</sub> exhibits insulating characteristics with a direct bandgap of 7.377 eV whereas its bulk form has an indirect bandgap of 7.02 eV. It means that when reducing the dimensionality of the MgCl<sub>2</sub> materials than its bandgap significantly increased. The optical properties of the monolayer MgCl<sub>2</sub> have been investigated using DFT within the random phase approximation. The calculated refractive index values are very near to water, which means that monolayer MgCl<sub>2</sub> material will be a transparent material. Also, the optical absorption coefficient is found to be very high in the ultraviolet (UV) region. From optical properties, the out-of-plane (E<math>\perp</math>Z) direction of polarizations is shifted towards the higher photon energy as compared to the in-plane (E<math>\parallel</math>X) direction. From the optical properties profile, the polarizations along in-plane and out-of-plane are different therefore it shows anisotropic behavior. These investigated results show the monolayer MgCl<sub>2</sub> could be a promising material for optoelectronic nanodevices such as deep UV emitters and detectors, electrical insulators, atomically thin coating materials.</p>
30.	<p><a href="#">Floor displacement-based torsional amplification factors for seismic design of acceleration-sensitive non-structural components in torsionally irregular RC buildings</a>  A Jain, M Surana - Engineering Structures, 2022</p> <p><b>Abstract:</b> In this study, the effects of inherent building torsion on the seismic response of acceleration-sensitive non-structural components are investigated. To achieve this objective, a group of elastic torsionally irregular step-back reinforced concrete moment-resisting frame buildings are analyzed under bi-directional earthquake excitations. The floor torsional amplification factors, defined as the ratio between the floor spectral ordinate at the flexible/stiff edge to the floor spectral ordinate at the center of rigidity, are obtained as a function of the tuning ratio for varying damping ratios of non-structural components. The correlations of the peak torsional amplification factors at different floors for the rigid and flexible non-structural components are studied with their floor displacement-based torsional irregularity indices, recommended in the national building codes of the United States and India. It is observed that</p>



	<p>the torsional amplification factors are building characteristics and tuning ratio-dependent. These torsional amplification factors are further observed to be well-correlated with the corresponding floor displacement-based torsional irregularity indices for both the rigid and flexible non-structural components. Contrarily, the torsional amplification factors for the very flexible non-structural components tend to unity and are thereby observed to be independent of the characteristics of both the building and the non-structural components. Simplified and numerically validated, floor displacement-based models are proposed to compute the torsional amplification factors, which can be used in aggregation with the existing codes to design acceleration-sensitive non-structural components in torsionally irregular buildings.</p>
31.	<p><a href="#">Graphitic carbon nitride for organic transformation (Chapter 13)</a>  <a href="#">S Samanta, R Srivastava - Nanoscale Graphitic Carbon Nitride, 2022</a></p> <p><b>Abstract:</b> Graphitic carbon nitride (g-C<sub>3</sub>N<sub>4</sub>) is emerging as a versatile catalyst and photocatalyst. The facile, one-step thermal-induced synthesis recipe, high thermal, and physical stability, chemical inertness, and semiconductor nature make it one of the most studied photocatalysts. Its excellent visible light harnessing capacity and appropriate band straddling to tackle the thermodynamic barriers for water splitting reaction also endow its excellent activity in photocatalytic reactions for the fine chemical synthesis. C<sub>3</sub>N<sub>4</sub> is a 2-dimensional material, constructed through the polymerization of multiple melem units, and connected via the N-N bond of adventitious N atoms of uncondensed amine groups. The N atoms in the melem framework and uncondensed amine groups induce Lewis basicity that demonstrates its versatility in thermal-induced catalysis besides photocatalysis. Moreover, the nonmetal doping (B, C, N, O, F, P, and S) in the bulk g-C<sub>3</sub>N<sub>4</sub> enables it to recognize as a versatile heterogeneous catalyst for numerous chemical reactions. The Lewis basicity and surface hydroxyl groups present on the surface of g-C<sub>3</sub>N<sub>4</sub> play pivotal roles in gas/reactants adsorption, and therefore make it a powerful candidate to trigger several catalytic reactions. The surface accessible sites can be appropriately tuned via surface exfoliation, vacancy creating, precursor alteration, mesoporosity introduction, and so on. In this chapter, a comprehensive understanding regarding the liquid-phase catalytic reactions catalyzed by g-C<sub>3</sub>N<sub>4</sub> in conventional thermal catalysis and light-induced pathways is presented. Moreover, to improve the catalytic activity and widen the application window of g-C<sub>3</sub>N<sub>4</sub>, several g-C<sub>3</sub>N<sub>4</sub>-based heterostructures have been developed to catalyze the organic transformations and such studies have also been discussed in this chapter. Overall this chapter is a balanced summary of the fundamentals and applications of g-C<sub>3</sub>N<sub>4</sub>, which would be interesting for students and researchers.</p>
32.	<p><a href="#">Gravitational lensing for stationary axisymmetric black holes in Eddington-inspired Born-Infeld gravity</a>  <a href="#">MS Ali, S Kauhsal - Physical Review D, 2022</a></p> <p><b>Abstract:</b> Recent years have witnessed a surge of interest of the lensing of the black holes arising from general as well as other modified theories of gravity due to the experimental data available from the Event Horizon Telescope (EHT) results. The EHT may open a new door indicating the possible existence of the rotating black hole solutions in modified theories of gravity in the strong field regime. With this motivation, we investigate in the present paper the equatorial lensing (<math>\theta=\pi/2</math>) by a recently obtained exact rotating black holes solution in Eddington-inspired Born-Infeld (EiBI) theory in both the strong- and weak-field limits. Such black holes are the modification of Kerr-Newman black holes in general relativity, characterized</p>

	<p>by their mass <math>M</math>, the charge <math>Q</math>, and the rotation parameter <math>a</math>. and an additional term <math>\varepsilon</math> accounting for the correction to the Kerr-Newman solutions. We show numerically the variations of the impact parameter <math>u_m</math>, the light deflection coefficients <math>p</math> and <math>q</math>, and the total azimuthal bending angle <math>\alpha D</math> and find a close dependence of these quantities on the charge parameter <math>r_q</math>, the correction term <math>\varepsilon</math>, and the spin <math>a</math>. We also calculate the angular position <math>\theta_\infty</math>, the angular separation <math>s</math>, and the magnification of the relativistic images. In addition, we also discuss the weak lensing of the black holes in Eddington-inspired Born-Infeld (EiBI) theory using the Gauss-Bonnet theorem. We calculate the weak lensing parameter and find its variation with different values of the parameters <math>r_q</math> and <math>\varepsilon</math>.</p>
33.	<p><a href="#">Influence of elastic instability and elastic turbulence on mixed convection of viscoelastic fluids in a lid-driven cavity</a>  S Gupta, A Chauhan, C Sasmal - International Journal of Heat and Mass Transfer, 2022</p> <p><b>Abstract:</b> The addition of a minute amount of solid polymers into a Newtonian solvent like water can originate an elastic instability as the Weissenberg number (ratio of the elastic forces to that of the viscous forces) gradually increases. These instabilities further transit to elastic turbulence (ET) regime at high Weissenberg numbers. In this study, we investigate how these elastic instabilities and elastic turbulence would tend to influence the mixed convective heat transfer phenomena in a lid-driven cavity, which is one of the widely studied problems in the domain of transport phenomena. In doing so, extensive two-dimensional time-resolved numerical simulations have been conducted by using an open-source CFD code OpenFOAM. The Oldroyd-B viscoelastic constitutive model is used in this study to realize the rheological behaviour of a constant shear-viscosity viscoelastic fluid or the so-called Boger fluid. To investigate the effect of the shear-thinning behaviour of a viscoelastic fluid on the elastic instability and elastic turbulence phenomena, we have further conducted limited simulations using the FENE-P (finitely extensible non-linear elastic spring with the Peterlin's approximation) viscoelastic fluid model. A detailed discussion is presented on how the flow dynamics and heat transfer mechanism inside the cavity can be influenced by the Weissenberg number along with the Reynolds, Prandtl, and Richardson numbers. We show that the heat transfer rate inside the cavity can be increased by more than 100% under appropriate conditions if one uses a constant shear-viscosity Oldroyd-B fluid instead of a simple Newtonian fluid due to the presence of elastic instability and elastic turbulence in the former fluid. Furthermore, we have found that the shear-thinning behaviour of a FENE-P viscoelastic fluid tends to suppress these instabilities and turbulence and hence decreases the heat transfer rate inside the cavity. Therefore, one can use the present approach of using a constant shear-viscosity Oldroyd-B fluid as an efficient way to increase the rate of heat and mass transport processes in various systems. Our approach can be served as an alternative possibility to the existing approaches such as the application of an electric or a magnetic field or the use of a nanofluid. However, one needs to be careful in the selection of the polymer type and its degradation behaviour as well as its appropriate concentration in the solution when choosing this approach.</p>
34.	<p><a href="#">Influence of Vermicompost as the Source of Nitrogen in Various Combinations with Chemical Fertiliser on Winter Wheat Productivity</a>  S Karmakar, D Kashyap - ASM Science Journal, 2021</p> <p><b>Abstract:</b> There is rarely any study that deals with the application of vermicompost in combination with chemical fertiliser to study the growth and yield variables of wheat crop in the</p>

	<p>typical agro-climatic conditions of saline sandy agricultural land of tropical semi-arid climatic condition with vast fluctuations of temperature between summer and winter seasons. Hence, the current study has been planned with a broader objective of utilising the organic resources by preparing vermicompost and applying it as the partial substitute of chemical fertiliser to cultivate wheat in an eco-friendly manner in saline sandy agricultural land of the tropical semi-arid zone. For achieving the intended goal, an experiment was conducted in the field of ‘Soil-Water-Plant Laboratory’, Department of Civil Engineering, IIT Ropar, Punjab, India during the winter season (rabi) of 2018-19. In this experiment, Randomized Block Design (RBD) was followed, and four treatments were used, including T1: 100% RD using chemical fertilisers, T2: 50% RD using chemical fertilisers + 50% of nitrogen through vermicompost, T3:75% RD using chemical fertilisers + 25% of nitrogen through vermicompost and T4: control (without any additional nutrients). Each treatment was replicated nine times. Plot size was 4m × 6m, and row to row spacing was 0.2 m. Following statistical analysis, it was found that treatment T2 (50% RD using chemical fertilisers + 50% of nitrogen through vermicompost) showed the best results, which were reflected in different parameters such as number of effective tillers per plant, ear length, number of grains per ear, and test weight, grain yield and straw yield of the wheat crop in comparison to other treatments. In this case, an almost equal amount of nitrogen supply from both organic and inorganic sources is responsible for getting the best results.</p>
35.	<p><a href="#"><u>Integrated RAN to Meet the QoS of Modern Wireless Application</u></a>  SK Singh, R Singh, B Kumbhani - IEEE 16th International Conference on Industrial and Information Systems, 2021</p> <p><b>Abstract:</b> The forthcoming wireless world is expected to have a variety of applications including massive IoT devices, vehicular communication, high-quality gaming, etc. Due to distinct Quality of Service (QoS) requirements, these applications demand different size of band-width and often possess significant variations in the working. Therefore, it is challenging for the existing cellular infrastructures to support such wide range of applications. On the other hand, there are some wireless technologies that are still underutilized, e.g., Narrow-Band Internet of Things (NB-IoT). To fill this gap, we propose a an integrated Cloud Radio Access Network (CRAN) architecture. Specifically, this work integrates the existing CRAN architecture with the NB-IoT. CRAN supports Coordinated Multi-Point (CoMP) transmission. So, the proposed integrated scheme intends to utilize full potential of microwave and mm-wave. Moreover, simulation results show that our proposed architecture suitably provides a better quality of Service (QoS) to all respective users.</p>
36.	<p><a href="#"><u>Investigating the effect of vacuum impregnation of supercapacitor electrode in electrolyte</u></a>  K Chatterjee, PK Agnihotri, N Gupta - IEEE 5th International Conference on Condition Assessment Techniques in Electrical Systems, 2021</p> <p><b>Abstract:</b> Supercapacitors provide much higher power density than conventional batteries, while providing comparable energy density. Generally, porous materials like activated carbon, carbon nanotubes etc. are used to fabricate supercapacitor electrodes. A critical factor influencing the performance of the supercapacitor is the effective surface area of the porous electrode accessed by the electrolyte ions. The electrode micro-structure, the size of the electrolytic ions, etc. influence the effective surface area. It is hypothesized that due to the presence of air bubbles in the finer pores of the electrode, the electrolyte ions are unable to access the electrode surface easily. In the present work, the effect of vacuum impregnation of the electrode in improving the</p>

	<p>effective surface area is investigated. Activated carbon-based supercapacitor electrodes are fabricated and characterized by electrochemical techniques, before and after vacuum impregnation. Vacuum impregnation is seen to result in higher energy density but lower power density, and this is thought to be linked to easier access to deeper and finer pores on the electrode surface.</p>
37.	<p><a href="#">J integral and local strain energy density approach to characterize the cracks in anisotropic hyperelastic skin type composite materials</a>  A Baranwal, PK Agnihotri - <i>Theoretical and Applied Fracture Mechanics</i>, 2022</p> <p><b>Abstract:</b> It has been proposed that the response of soft tissues and skin type materials critically depends on the orientation and re-orientation of reinforcing fiber. Here, we quantify the effect of fiber orientation on the mechanical and fracture properties of anisotropic hyperelastic glass fiber (GF)/polydimethylsiloxane (PDMS) composites through a unified experimental and computational analysis. Experimental results show that the tensile strength and fracture toughness of skin type materials depends on the initial orientation of fiber families and is maximum for 0–90 fiber orientation. The re-orientation of fibers under tensile loading is experimentally demonstrated. The experimental findings are well complimented by the finite element (FE) simulations performed using bilinear strain stiffening fiber and matrix (BLFM) material model for soft tissues. The material model parameters are obtained by fitting the experimental data for a meaningful comparison. It is observed that fiber rotation along the loading direction indeed enhances the resistance to crack growth in skin type materials. The size of process zone (RC) ahead of the crack tip and relative contribution of anisotropic energy is characterized using J integral and average strain energy density (ASED) criteria. The RC and anisotropic energy contribution (<math>\phi_{\text{aniso-avg}} / \phi_{\text{avg}}</math>) depends on the fiber orientation with higher values for 0–90 fiber orientation. The larger process zone enhances the fracture toughness for 0–90 orientation in comparison to other orientations. Moreover, RC and <math>\phi_{\text{aniso-avg}} / \phi_{\text{avg}}</math> are found to be independent of initial crack length and therefore, they can be considered as material parameters for a given fiber orientation. The findings of the present investigations may be used to explore GF/PDMS composite as a possible candidate for soft actuator and bio-medical applications with enhanced toughness.</p>
38.	<p><a href="#">Load Frequency Control of Two Area Microgrid Using Reinforcement Learning Controller</a>  S Beura, DK Soni, BP Padhy - <i>9th IEEE International Conference on Power Systems</i>, 2021</p> <p><b>Abstract:</b> In this paper, automatic generation control problem is inspected and different modelling parameters are decided. Initially Genetic algorithm (GA) based parameters of proportional-integral-derivative (PID) controller is applied to the model. Then Q learning (Reinforcement learning) applied to control the frequency and tie line power deviation by controlling the power mismatch between generators and loads. Area control error (ACE) are used as objective function for PID and RL controller respectively. Q-learning based reinforcement agent is introduced which takes the action according to averaged ACE values. Parameters like step size, discount rate, and exploration rate decides the effectiveness of the RL scheme.</p>
39.	<p><a href="#">Machinability Analysis During Laser Assisted Turning of Aluminium 3003 Alloy</a>  N Deswal, R Kant - <i>Lasers in Manufacturing and Materials Processing</i>, 2022</p> <p><b>Abstract:</b> Laser assisted turning (LAT) is emerging as a significant process for machining various materials. In this study, experimental analysis is carried out to investigate the</p>

	<p>machinability of the aluminium 3003 alloy during conventional turning (CT) and LAT processes. The effect of laser beam irradiation on machining performance is analyzed and compared with the CT in terms of machining forces, chip morphology, and surface roughness. The results showed that in comparison with CT, the cutting, thrust, and feed forces could be reduced significantly in LAT. However, these forces were found to be increased at other than optimum laser power. It was pretty interesting to observe that the cutting, thrust, and feed forces were increased at high laser power. Surface roughness was also found to be higher in LAT than that in CT. Chip morphology analysis showed that the discontinuous and thick chips are observed at high laser power, whereas continuous and small chips are observed at low laser power, while continuous and long chips are obtained for CT. The presented results are important for manufacturing industries seeking to improve the machinability of the materials.</p>
40.	<p><a href="#">Mapping Environmental Impacts of Rapid Urbanisation and Deriving Relationship between NDVI, NDBI and Surface Temperature: A Case Study</a>  V Saini - IOP Conference Series: Earth and Environmental Science, 2021</p> <p><b>Abstract:</b> Urbanisation is a complex global phenomenon driven by unorganised expansion, increased immigration, and population explosion. Changes in land cover are one of the most critical components for managing natural resources and monitoring environmental impacts in this context. In the present study, a hybrid classification approach was applied to Landsat data to get insight into the urbanisation of the Chandigarh capital region from 2000 to 2020. The results demonstrate an increasing urbanisation tendency on the city's outskirts, particularly in the north-western and southern directions. The most considerable alterations were seen in the class vegetation as it swiftly transformed to built-up regions. Two indices, namely NDVI and NDBI and surface temperature images, were also derived from studying their inter-relationships. The paper suggests a positive linear relationship between surface temperature and NDBI while a negative correlation between NDVI and NDBI. Such studies may help city planners to take timely and appropriate efforts to reduce the environmental consequences of urbanisation.</p>
41.	<p><a href="#">Multispectral Image Demosaicking based on Novel Spectrally Localized Average Images</a>  V Rathi, P Goyal - IEEE Signal Processing Letters, 2021</p> <p><b>Abstract:</b> In this letter, we propose a new generic multispectral image demosaicking algorithm using adaptive spectral correlation. Our proposed algorithm defines the spectrally localized average image (SLAI) corresponding to each spectral band, which has a strong spectral correlation with the pixel values of the corresponding spectral band in the raw image captured using a single sensor. The proposed algorithm uses the SLAI to estimate the missing pixel values of the spectral bands. Experimental results reveal that our algorithm outperforms other state-of-the-art generic multispectral image demosaicking algorithms in terms of objective and subjective evaluations.</p>
42.	<p><a href="#">Nanomechanical properties of human hair using AFM, nanoindentation, SEM and EDX</a>  Avinash, M Mursaleen, N Kumar, P Sihota - Jurnal Tribologi, 2021</p> <p><b>Abstract:</b> Human hair is a natural fiber which is having a composite structure. The nanomechanical properties of human hair can be altered in pathological conditions, and small scale characterization of human hair can be helpful to estimate these changes of material and compositional properties. The paper presents the study of small scale properties of human hair including surface roughness, elastic modulus, hardness, surface morphology, sulphur content</p>



using Atomic force microscopy, nanoindentation, scanning electron microscopy and energy dispersive x-ray spectroscopy. The observations on studying both the control and thyroid hair depicted increase roughness, decreased material properties, decreased sulphur content and altered surface morphology in thyroid group as compared to control hair.

[Novel imidazo \[1, 2-a\] pyridine derivatives induce apoptosis and cell cycle arrest in non-small cell lung cancer by activating NADPH oxidase mediated oxidative stress](#)

K Bhavya, M Mantipally, S Roy, L Arora, VN Badavath...D Pal - Life Sciences, 2022

**Abstract:**

**Aims**

Imidazo[1,2-a]pyridine-based analogues have recently gained significant interest because of their wide spectrum of biological activities including anti-cancer potential, however the development of targeted therapeutic candidates against non-small cell lung cancer (NSCLC) is of utmost need due to its high prevalence and poor prognosis. Herein, we have aimed to synthesized novel imidazo [1,2-a] pyridine derivatives (IMPA) by coupling with 2-amino-4H-pyranto enhance bioactivity against NSCLC.

**Main methods**

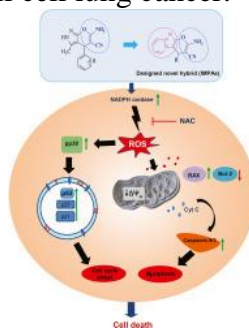
We have designed and synthesized a series of fifteen novel imidazo [1,2-a] pyridine derivatives through molecular hybridization and studied their anti-cancer activity against in-vitro lung adenocarcinoma and 3D multicellular lung tumor spheroids.

**Key findings**

43. IMPA-2, IMPA-5, IMPA-6, IMPA-8, and IMPA-12 markedly induced cytotoxicity by notably increased NADPH oxidase (NOX) activity, which results in the induction of ROS-mediated apoptosis in A549 lung cancer cells. It caused impairment of mitochondrial membrane potential by increasing pro-apoptotic BAX, and BAK1 expressions, and decreasing anti-apoptotic BCL2 expression, along with the induction of caspase-9/3 activation, however, these attributes were compromised in presence of N-acetyl-L-cysteine (NAC), a free radical scavenger. Increased ROS production by IMPAs also promotes p53 mediated cell cycle arrest through the inactivation of p38MAPK. Reduction of tumor size in IMPAs-treated 3D multicellular lung tumor spheroids gave further validation.

**Significance**

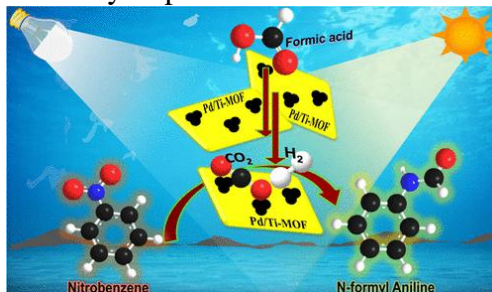
Beside cytotoxicity, IMPAs also inhibit lung cancer cell invasion and migration, suggesting their applicability in metastatic lung cancer. Therefore, IMPA derivatives could be used as potential anti-cancer agents in treating non-small cell lung cancer.



44.	<p><a href="#">Numerical simulations for electro-osmotic flow of PTT fluids in diverging microchannel</a>  M Trivedi, S Maurya, N Nirmalkar - Materials Today: Proceedings, 2022</p> <p><b>Abstract:</b> In the current work, the electroosmotic coupled pressure driven flow through a diverging microchannel has been numerically investigated for the simplified Phan Thien Tanner (PTT) fluids. The Debye-Hückel approximation is used for the linearization of electric potential distribution in the electric double layer and the Debye length has been kept fixed (<math>\kappa H = 20</math>). The pressure and electroosmotic forces are coupled and by, <math>\Gamma</math>, the forcing ratio (the ratio of pressure to the electrokinetic gradient in the direction of flow), which is varied in the range of <math>-4 \leq \Gamma \leq 4</math>. The viscoelastic fluid rheology has been modulated by the combined effect of the characteristic Deborah number and the PTT parameter as <math>0.1 \leq \varepsilon De \leq 5</math>. The influence divergent angle (<math>5^\circ \leq \alpha \leq 15^\circ</math>) has also been demonstrated to analyze the role of channel geometry on the resulting flow kinematics. The resulting variations in the flow field have been presented and discussed in the form velocity vectors, surfaces and velocity profiles at the outlet of the channel.</p>
45.	<p><a href="#">On De la Vallée Poussin means for harmonic mappings</a>  AS Kaliraj - Monatshefte für Mathematik, 2022</p> <p><b>Abstract:</b> In this article, we study the geometric properties of <math>V_n(f)</math>, the <math>n^{\text{th}}</math> De la Vallée Poussin means for univalent starlike harmonic mappings <math>f</math>. In particular, we provide a necessary and sufficient condition for <math>V_n(f)</math> to be univalent and starlike in the unit disk <math>D</math>, when <math>f \in S^*_H</math>, the class of all normalized univalent starlike harmonic mappings in <math>D</math>. We determine the radius of fully starlikeness (respectively, fully convexity) of <math>V_2(f)</math>, when <math>f \in S^0_H</math> and the result is sharp. Then, we determine the radius <math>r_n \in (0,1)</math> so that <math>V_n(f)</math> is univalent and fully starlike in <math> z  &lt; r_n</math>, whenever <math>f</math> is univalent and fully starlike harmonic mapping in <math>D</math>. We also discuss about the geometry preserving nature of <math>V_n(f)</math>, when <math>f</math> belongs to some well known geometric subclasses of <math>S_H</math>.</p>
46.	<p><a href="#">On the convective mass transfer and flow across spherical droplet falling in Casson fluids</a>  MJ Alam, A Sharma, M Trivedi, N Nirmalkar - Materials Today: Proceedings, 2022</p> <p><b>Abstract:</b> In this work, we have investigated the flow and mass transfer across spherical droplet falling in the non-Newtonian fluids (Casson fluids). For the different values of dimensionless parameters like Reynolds number; <math>1 \leq Re \leq 100</math> Bingham number; <math>0 \leq Bn \leq 50</math>, viscosity ratio; <math>0.1 \leq \kappa \leq 10</math>, and Schmidt number; <math>Sc = 10</math>. The governing equation of momentum and mass transport is solved numerically with Casson constitutive equation and appropriate boundary conditions. To prevent singularity in the Casson model, the Papanastasiou regularization model is introduced. Local transport properties are shown by streamlines and concentration contours, and average transport parameters, such as the Sherwood number, are presented over the surface of the droplet. Yielded and un-yielded zone were observed to coexist inside the flow domain due to the fluid-yield stress. The convective mass transfer was observed in the yielded fluid region while the un-yielded area is dominated by molecular diffusion. Furthermore, as value of Bingham number increases, the un-yielded area dominates, and yielded areas progressively disappear.</p>
47.	<p><a href="#">On the scattering and radiation of water waves by a finite dock floating over a rectangular trench</a>  A Choudhary, K Trivedi, S Koley, SC Martha - Wave Motion, 2022</p> <p><b>Abstract:</b> In this study, the scattering and radiation of surface water waves by a finite dock</p>

	<p>floating over an asymmetric rectangular trench-type bottom topography are analyzed. The boundary value problems are handled for solutions analytically using a matched eigenfunction expansion method and numerically using the boundary element method. Various physical quantities associated with the scattering and radiation problems are studied for various values of wave and structural parameters. The results demonstrate that the scattering coefficients are significantly influenced due to the variation in dock length and depth ratios of the bottom trench. In the case of radiation problems, the dock length plays a crucial role in analyzing the radiation coefficients and wave excitation forces associated with each mode of motion. On the other hand, the effect of depth ratios of the bottom trench is negligible on the radiation coefficients. The present study reveals that the scattering of water waves by a floating dock over an abrupt change in bottom topography plays an important role in the construction of floating structures having more durability to resist harsh wave environments and reduce the wave impact near the seashore.</p>
48.	<p><a href="#">Organic Cation Receptor for Colorimetric Lateral Flow Device: Detection of Zearalenone in Food Samples</a>  M Kumar, G Singh, N Kaur, N Singh - ACS Applied Materials &amp; Interfaces, 2022</p> <p><b>Abstract:</b> As per the WHO reports, it has been estimated that almost 25% of food crops contain mycotoxins as the major contaminant. In this work, we developed a paper-based colorimetric lateral flow device (CLFD) impregnated with an organic cation receptor (OCR) for sensitive and selective detection of zearalenone (ZEN). Various techniques such as ultraviolet (UV)–visible absorption, cyclic voltammetry, and fluorescence spectroscopy were used for the detection of mycotoxins, and it was observed that OCR shows sensitivity and selectivity toward zearalenone (ZEN) only, irrespective of any other analytes. Furthermore, the colorimetric test revealed that the developed OCR shows a change in color with the addition of ZEN from greenish-gray to blue that is visible to the naked eye. The quantification of ZEN was also achieved using RGB analysis and compared with UV–visible spectroscopy data. Further, for the on-site detection of ZEN, a paper-based CLFD was also developed and used to evaluate the spiked corn sample containing ZEN, and it provided significant results with a limit of detection (LOD) of 0.31 nM (3<math>\sigma</math> method), good linearity (<math>R^2 = 0.9702</math>), good reproducibility (<math>SD = \pm 6\%</math>, triplicate), and good recovery of ZEN of 95–102% with a variation coefficient (VC) varying from 1.56 to 4.62%. Therefore, the device has the potential to check the mycotoxin toxicity in food products and is helpful in remote and developing areas.</p>
49.	<p><a href="#">Pd-Embedded Ti Metal–Organic Framework Nanostructures for Photocatalytic Reductive N-Formylation of Nitroarenes in Water</a>  AK Kar, A Behera, R Srivastava - ACS Applied Nano Materials, 2022</p> <p><b>Abstract:</b> The photocatalytic reductive N-formylation of nitroarenes is carried out over a Pd nanoparticle (Pd NP)-embedded nanostructured Ti-metal–organic framework (MOF) using sunlight or a household white light-emitting diode (LED). Herein, the Ti-MOF is used as a visible-light-absorbing material, and the Pd NPs boost the photogenerated charge-carrier separation and transfer to the active sites for catalyzing the photocatalytic N-formylation of nitroarenes. The surface characteristics, oxidation states, and elemental compositions of the nanostructured materials were characterized by several physicochemical characterization techniques. Optical property and photoelectrochemical measurements were conducted to determine the bandgap, electron–hole recombination rate, band edge potentials, photocurrent density, charge-carrier separation, and so on. N-formylation of nitroarenes was achieved using</p>

HCOOH as a sustainable hydrogen and formylating source with simple household white LED bulbs. The yield of N-formylated arene was excellent in an aqueous medium. The structure–activity relationship was revealed using photocatalytic activity data, physicochemical and optoelectronic characteristics, control experiments, and scavenging studies. The high photocatalytic performance of the Pd/Ti-MOF can be ascribed to the direct contact between the Pd NPs and MOF, the generation of abundant catalytically active sites, and the superior electrical conductivity that leads to rapid electron transfer processes. The Pd/Ti-MOF exhibited excellent photostability and recyclability. The efficient catalyst design, an economical and sustainable light source for the direct formylation of nitroarenes, would attract researchers to develop similar catalytic protocols to other industrially important chemicals.



[Performance analysis of a solar still driven by a packed bed thermal storage tank during off-sunshine period](#)

S Verma, R Das - *Journal of Energy Storage*, 2021

50.

**Abstract:** During cloudy or rainy days, when sunlight is absent, a solar still cannot operate in its natural mode. In such circumstances, the still can be run using energy stored in thermal storage systems during sunshine hours. This work presents an analytical investigation of such a scenario in which a packed bed sensible thermal storage tank is used to provide the input energy for desalination via a double basin solar still during off sunshine season. Closed form solutions are derived for the temperature profile in storage tank, and of temperatures in both upper and lower basins of the still. Using these solutions, a closed form solution is obtained for the net mass of distillate produced until the cessation of operation. Parametric studies reveal that the present system can produce appreciable quantity of pure water that remains unchanged with any variation in mass of water in either basin of the double basin still,  $m_{w1}$ ,  $m_{w2}$ . The net distillate increases linearly with an increase in the initial tank excess temperature,  $\theta_0$ . Further, the analysis tells that there is optimum mass flow rate of the working fluid that delivers heat from storage tank to the still,  $m'$  that maximizes net distillate production. The reason of existence of such an optimum mass flow rate is discussed in detail. For the values considered, it is seen that a storage tank of 1 m<sup>3</sup> vol, at an initial temperature of 50 °C above ambient, can produce 11.69 kg of potable water, yielding a thermal efficiency of about 68%. This work is a first ever investigation of the viability of a packed bed thermal storage tank for operating a solar still, and can serve as a guiding study for further, more comprehensive research work in this direction.

[Phase locking of lasers with Gaussian coupling](#)

ANK Reddy, S Mahler, A Goldring, V Pal... - *Optics Express*, 2022

51.

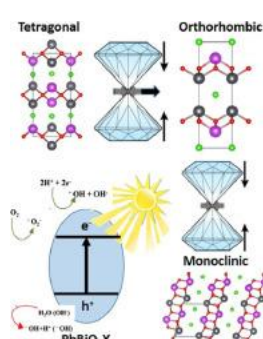
**Abstract:** A unique approach for steady in-phase locking of lasers in an array, regardless of the array geometry, position, orientation, period or size, is presented. The approach relies on the

insertion of an intra-cavity Gaussian aperture in the far-field plane of the laser array. Steady in-phase locking of 90 lasers, whose far-field patterns are comprised of sharp spots with extremely high power density, was obtained for various array geometries, even in the presence of near-degenerate solutions, geometric frustration or superimposed independent longitudinal modes. The internal phase structures of the lasers can also be suppressed so as to obtain pure Gaussian mode laser outputs with uniform phase and overall high beam quality. With such phase locking, the laser array can be focused to a sharp spot of high power density, useful for many applications and the research field.

52. [Pressure induced structural phase transition and piezochromism in photovoltaic sillen compounds  \$PbBiO\_2X\$  \(X= Cl, Br & I\)](#)  
 A Majumdar, R Ahuja - Applied Materials Today, 2022

**Abstract:** Hydrostatic pressure is an effective and clean method that can give rise to the emergence of novel crystal structures and physical properties. Thus, hydrostatic pressure can be used for designing new functional materials. Sillen materials or  $PbBiO_2X$  (X = Cl, Br & I) are a class of materials which have gained considerable interest in the field of ferroelectrics, photocatalysis, etc. In this work, we have used first principles methods to predict the crystal structure and phase of sillen materials at different pressure points from 0 to 50 GPa. It was then followed by the study of their structural, electronic and optical properties upon compression. Upon compression, the band gaps decreased within a particular phase and showed kinks on phase transitions. In the compressed states, the band gaps are in the suitable range to be used in the visible range of the spectrum for photovoltaic properties. Piezochromism is also reported upon compression as can be seen from the changes in the optical absorption spectra. This work should remove any confusion with regards to the responsible phase at different pressures, and the possible existence of new phases with the respective band gaps should pave the way for future experimental works on photocatalysis and other energy applications.

**Graphical Abstract:**



The graphical abstract illustrates the structural phase transition of  $PbBiO_2X$  under pressure. It shows three crystal structures: Tetragonal, Orthorhombic, and Monoclinic. The transition from Tetragonal to Orthorhombic is indicated by a downward arrow, and from Orthorhombic to Monoclinic by a downward arrow. A schematic diagram shows the band structure of  $PbBiO_2X$  with the conduction band (CB) and valence band (VB) separated by a band gap. Light excitation promotes electrons from the VB to the CB, creating electron-hole pairs ( $e^-$  and  $h^+$ ). A photocatalytic reaction is shown:  $2H_2O + 2h^+ \rightarrow H_2 + O_2$ .

53. [Prioritization and ranking of lean practices: a case study](#)  
 NR Sangwa, KS Sangwan - International Journal of Productivity and Performance Management, 2022

**Abstract:**  
 Purpose  
 The paper aims to identify, prioritize and rank lean practices in the context of an Indian automotive component manufacturing organization using interpretive ranking process (IRP) and



	<p>interpretive structural modeling (ISM) approaches.</p> <p><b>Design/methodology/approach</b> Lean practices are identified from the literature. Then, two hierarchical models were developed using two distinct modeling approaches – ISM and IRP with expert opinions from an Indian automotive component manufacturing organization to analyze the contextual relationships among the various lean practices and to prioritize and rank them with respect to performance dimensions.</p> <p><b>Findings</b> In the study, the hierarchical structural models are developed using ISM and IRP approaches for an Indian automotive component manufacturing organization. In ISM-based modeling, lean practices can be categorized into five levels. Top priority should be given to the motivators followed by value chain, system/technology and organization centric practices. IRP model shows the dominance relationship among the various lean practices with respect to performance dimensions.</p> <p><b>Practical implications</b> The models are constructed from the organizational standpoint to evaluate their impact to the implementation of lean manufacturing. The study leverages the organizations to prioritize limited resources as per the hierarchy. Managers get the inter-linkages and ranking of various lean practices, which leads to a better perspective for the effective implementation of lean. The structural models also assist management to assign proper roles to employees/departments for effective lean implementation.</p> <p><b>Originality/value</b> There is hardly any structural model of lean practices in the literature for clustering, prioritizing and ranking of lean practices. The study fills this gap and develops the hierarchical models of lean practices through IRP and ISM approaches for an Indian automotive component manufacturing organization. The results from both approaches are compared for illustrating the benefits of one over the other.</p>
54.	<p><a href="#"><u>Quantum Cost-Efficient Design of Synchronous Reversible Shift Registers using Reversible Logic</u></a> S Gupta, R Kumar, S Kumar - IEEE Bombay Section Signature Conference, 2021</p> <p><b>Abstract:</b> Reversible circuits are one of the most promising technologies for replicating inputs from recorded outputs, and it results in lower power dissipation. All gates such as NAND, AND, OR, NOR etc. are irreversible in nature and consume energy during calculations. Similar to quantum circuits, reversible logic circuitry does not consume energy throughout the calculation cycle. Due to this, reversible circuits can be used for quantum communication and other low-power applications. Registers are one of the most important storage components utilised in a wide range of real-time operations. Using expressions of exclusive-or sum of products (ESOP) and modified Fredkin gates, this work presents a novel way for creating a quantum cost-effective universal register circuit. The designed universal register circuitry for left and right shifts are tested in the Xilinx Vivado simulator to ensure that they are functional and logically correct. The proposed universal registers outperform the standard designs in terms of garbage outputs (GO),</p>

	quantum cost (QC), gate count (GC), and Ancilla inputs (AI), according to the comparative analysis.
55.	<p><a href="#">Quantum interference effect in plasmonic transmission in the presence of quantum emitters</a> K Mehta, S Dasgupta - Journal of Modern Optics, 2021</p> <p><b>Abstract:</b> In this paper, we show how to enhance the transmission of the surface plasmon field using several interacting two-level quantum emitters placed in a plasmonic environment. Our model relies on quantum interference effect and, therefore, can be treated as a plasmonic analog of the electromagnetic induced transparency, usually referred to in the context of driven atomic systems. Moreover, our model with multiple interacting quantum emitters, similar to Ising spin chain, can be used for broadband transmission of the surface plasmon field.</p>
56.	<p><a href="#">Roles of Optical Phonons and Logarithmic Profile of Electron-Phonon Coupling Integration in Superconducting Sc<sub>0.5</sub>Y<sub>0.5</sub>H<sub>6</sub> Superhydride Under Pressures</a> W Sukmas, P Tsuppayakorn-aeak, U Pinsook, R Ahuja... - Journal of Alloys and Compounds, 2022</p> <p><b>Abstract:</b> The stable structure of symmetrically Sc/Y-substituted hexahydride Sc<sub>0.5</sub>Y<sub>0.5</sub>H<sub>6</sub> under high pressures is theoretically reported herein to superconduct with maximum T<sub>c</sub> of 127 K, as supported by analyses of the electronic band structure, Fermi surface topologies, phonon dispersion, and the Eliashberg spectral function. We also expatiate on an alternative approach in describing the nature of T<sub>c</sub> under pressures, i.e. the bandwidth function as an approximation of the spectral function (<math>\alpha^2F</math>) for Sc<sub>0.5</sub>Y<sub>0.5</sub>H<sub>6</sub>. Being a special case, the bandwidth function is derived from an analytic solution for the <math>\alpha^2F</math> function given constraints arising from the characteristics of the function itself. The consistency between the DFT-obtained <math>\alpha^2F</math> function and that of the proposed model suggests the dominant role played by the cutoff frequency for the optical modes in affecting T<sub>c</sub>.</p>
57.	<p><a href="#">Scheduling Real-Time Security Aware Tasks in Fog Networks</a> A Singh, N Auluck, O Rana... - IEEE Transactions on Services Computing, 2021</p> <p><b>Abstract:</b> Fog computing brings the cloud closer to a user with the help of a micro data center (mdc), leading to lower response times for delay sensitive applications. RT-SANE (Real-Time Security Aware scheduling on the Network Edge) supports batch and interactive applications, taking account of their deadline and security constraints. RT-SANE chooses between an mdc (in proximity to a user) and a cloud data center (cdc) by taking account of network delay and security tags. Jobs submitted by a user are tagged as: private, semiprivate and public, and mdcs and cdcs are classified as: trusted, semi-trusted and untrusted. RT-SANE executes private jobs on a user's local mdcs or pre-trusted cdcs, and semi-private and public jobs on remote mdcs and cdcs. A security and performance-aware distributed orchestration architecture and protocol is made use of in RT-SANE. For evaluation, workload traces from the CERIT-SC Cloud system are used. The effect of slow executing straggler jobs on the Fog framework are also considered, involving migration of such jobs. Experiments reveal that RT-SANE offers a higher "success ratio" (successfully completed jobs) to comparable algorithms, including consideration of security tags.</p>
58.	<p><a href="#">Sectoral Growth and Sectoral Credit: Panel Evidence from Indian States</a> S Bardhan, R Sharma - Revisiting the Indian Financial Sector, Part of the India Studies in Business and Economics book series, 2022</p>

	<p><b>Abstract:</b> The chapter examines the relationship between sectoral growth and sectoral credit across Indian states during last four decades. Findings based on system generalized method of moments estimations reveal that in the decades of 1980 and 1990, different credit components hardly had any effect on Indian states' sectoral growth. However, in the 2000s, financial intermediation exerts a positive and significant effect on economic growth, given that service sector credit witnessed the most significant spurt. Contrary to expectations, industrial credit did not affect sectoral growth in the 1990s following a significant deceleration in the industrial sector. However, following the revival of industrial sector in the decade of 2000 and the subsequent period under investigation, industrial credit played a significant role in growth process of states. The rapid growth in Indian economy in the 1990s has been primarily supported by service sector rather than industry. However, major policy concern lies in an optimal allocation of resources through efficient credit delivery mechanism and investment in infrastructure for sustained and balanced growth across sectors.</p>
59.	<p><a href="#">Shape coexistence and octupole correlations in <math>^{72}\text{Se}</math></a>  A Mukherjee, S Bhattacharya, T Trivedi, RP Singh... D. Choudhury... - Physical Review C, 2022</p> <p><b>Abstract:</b> In the present paper, we report the results from the study of excited states in the <math>^{72}\text{Se}</math> nucleus using the <math>^{50}\text{Cr}(^{28}\text{Si}, \alpha 2p)^{72}\text{Se}</math> fusion evaporation reaction at a beam energy of 90 MeV. The deexciting <math>\gamma</math> rays were detected using the Indian National Gamma Array (INGA). A total of ten new <math>\gamma</math>-ray transitions have been identified using the <math>\gamma</math>-<math>\gamma</math> coincidence technique. The <math>K^\pi=0^+_2</math> band based on an isomeric state has been extended up to a (10+) state at 5.473 MeV excitation energy, and four new interconnecting transitions have been placed between this band and yrast band. Further, the enhanced interconnecting E1 transitions between positive- and negative-parity bands suggest the existence of octupole correlations in this nucleus. The characteristics of the observed bands in the experiment have been interpreted in terms of the total Routhian surface (TRS) calculations.</p>
60.	<p><a href="#">Speak2label: Using domain knowledge for creating a large scale driver gaze zone estimation dataset</a>  S Ghosh, A Dhall, G Sharma... - Proceedings of the IEEE/CVF International Conference on Computer Vision Workshops, 2021</p> <p><b>Abstract:</b> Labelling of human behavior analysis data is a complex and time consuming task. In this paper, a fully automatic technique for labelling an image based gaze behavior dataset for driver gaze zone estimation is proposed. Domain knowledge is added to the data recording paradigm and later labels are generated in an automatic manner using Speech To Text conversion (STT). In order to remove the noise in the STT process due to different illumination and ethnicity of subjects in our data, the speech frequency and energy are analysed. The resultant Driver Gaze in the Wild (DGW) dataset contains 586 recordings, captured during different times of the day including evenings. The large scale dataset contains 338 subjects with an age range of 18-63 years. As the data is recorded in different lighting conditions, an illumination robust layer is proposed in the Convolutional Neural Network (CNN). The extensive experiments show the variance in the dataset resembling real-world conditions and the effectiveness of the proposed CNN pipeline. The proposed network is also fine-tuned for the eye gaze prediction task, which shows the discriminativeness of the representation learnt by our network on the proposed DGW</p>

	dataset.
61.	<p><a href="#">Stability analysis of power system connected to wind farm using Eigenvalue sensitivity approach</a> B Sahu, BP Padhy - 9th IEEE International Conference on Power Systems, 2021</p> <p><b>Abstract:</b> This paper presents a comprehensive idea about the eigenvalue sensitivity analysis in a renewable source based power system. This method renders very useful information about power system stability studies. Based on two axis model theory an explicit mathematical model of a four bus test system containing a Doubly Fed Induction Generator (DFIG) based wind farm is developed. The eigenvalue sensitivity analysis corresponds to first-order derivative of the reduced state transition matrix of the power system is performed with respect to various system operating parameters. In this research the system operating parameters taken under considerations are line impedance, real and reactive power loading. Finally, Hopf-Bifurcation margin curve is given for different critical parameters.</p>
62.	<p><a href="#">Stability criteria and convective mass transfer from the falling spherical drops, part II: Herschel-Bulkley fluids</a> MJ Alam, N Nirmalkar, AK Gupta - The Canadian Journal of Chemical Engineering</p> <p><b>Abstract:</b> The combined effects of yield stress, shear-thinning, and shear-thickening fluid behaviour are investigated when a drop is falling in a Herschel-Bulkley fluid. The constitutive relation for Herschel-Bulkley fluids is regularized using the Papanastasiou regularization method. The governing partial differential equations for mass, momentum, and species transport are solved spanning a wide range of dimensionless numbers as Reynolds number, <math>1 \leq Re \leq 150</math>; Schmidt number (10); Bingham number, <math>0 \leq Bn \leq 50</math>; viscosity ratio (0.1 and 10); and power-law index, <math>0.4 \leq n \leq 1.6</math>. The velocity field and mass transfer characteristics are expressed using streamlines, velocity contours, concentration contours, and sheared and un-sheared regions, while the surface averaged gross engineering quantities are described as a drag coefficient, yield-stress parameter, and Sherwood number. All else being equal, sheared regions in shear-thinning fluids are observed to be larger with respect to the shear-thickening fluids at finite Reynolds numbers. In the fully plastic flow limit, the yield stress effects dominate in the flow field, and therefore, the critical yield-stress parameter is observed to be independent of shear-thinning and shear-thickening fluid behaviour. However, in the viscoplastic limit (finite Bingham number), shear-thinning fluid always requires a larger value of yield stress to be static in the fluid with reference to shear-thickening fluids. The new set of dimensionless parameters are defined based on the effective viscosity scales and the predictive correlations are put forward for both drag coefficient and Sherwood number.</p>
63.	<p><a href="#">Sustainability assessment of crops' production in India: empirical evidence from ARDL-ECM approach</a> RR Chopra - Journal of Agribusiness in Developing and Emerging Economies, 2022</p> <p><b>Abstract:</b> Purpose The study aims to evaluate the long- vs short-run relationships between crops' production (output) and crops' significant inputs such as land use, agricultural water use (AWU) and gross irrigated area in India during the period 1981–2018.</p> <p>Design/methodology/approach</p>

	<p>The study applied the autoregressive distributed lag (ARDL) bounds testing approach to estimate the co-integration among the variables. The study uses the error correction model (ECM), which integrates the short-run dynamics with the long-run equilibrium.</p> <p><b>Findings</b> The ARDL bounds test of co-integration confirms the strong evidence of the long-run relationship among the variables. Empirical results show the positive and significant relationship of crops' production with land use and gross irrigated area. The statistically significant error correction term (ECT) validates the speed of adjustment of the empirical models in the long-run.</p> <p><b>Research limitations/implications</b> The study suggests that the decision-makers must understand potential trade-offs between human needs and environmental impacts to ensure food for the growing population in India.</p> <p><b>Originality/value</b> For a clear insight into the impact of climate change on crops' production, the current study incorporates the climate variables such as annual rainfall, maximum temperature and minimum temperature. Further, the study considered agro-chemicals, i.e. fertilizers and pesticides, concerning their negative impacts on increased agricultural production and the environment.</p>
64.	<p><a href="#">Switched Polarized H-Field Forming using a Planar Switchable Double-Dumbbell Coil Antenna for Orientation-Oblivion Wireless Power Transfer</a> VK Srivastava, A Sharma - IEEE Transactions on Antennas and Propagation, 2022</p> <p><b>Abstract:</b> A planar switchable multi-coil transmitter antenna is presented to eliminate angular misalignment problem in near-field wireless power transfer applications. To power the receiver antenna in any orientation, the previous methods of 3-D rotating H-field forming required complex feeding with multiple modulated sources. As an alternate, a switched polarized H-field is proposed which conjoins field-forming technique with switching control to exploit the orthogonal field components using a single excitation source. The switching periods and corresponding H-field components are controlled to satisfy analytically derived constraint for complete mitigation of the angular misalignment problem. To generate this switched polarized H-field, the proposed antenna comprises planar single axial and double dumbbell coils optimized to provide a maximum S21 with the receiver coil such that a maximum link efficiency is obtained under the field constraint. The switching is integrated with the design using two SPDT switches and a planar cost-effective realization in PCB technology is achieved. The proposed approach and the antenna is experimentally validated and the results are corroborated showing a constant voltage induced in the receiver coil with a standard deviation of 0.0028 V. The results proved the potential of the proposed switchable transmitter antenna generating switched polarized H-field for orientation-oblivion WPT applications.</p>
65.	<p><a href="#">Systematic study of fusion suppression for tightly bound projectiles at above-barrier energies</a> MS Asnain, M Shuaib, I Majeed, MK Sharma...PP Singh... - Physical Review C, 2022</p> <p><b>Abstract:</b> The present work aims to explore the effects of projectile breakup on fusion cross section at energies near the Coulomb barrier to well above it. The complete fusion cross section for the strongly bound non-<math>\alpha</math>-cluster projectile <math>^{14}\text{N}</math> in interaction with a <math>^{181}\text{Ta}</math> target was obtained by summing the experimentally measured channel-by-channel cross section data of evaporated</p>



	<p>residues. The obtained total fusion cross section was compared with the theoretical code cfull and the results were found to be consistent with each other. Further, the experimental fusion function data on <math>^{181}\text{Ta}</math> target with <math>^{14}\text{N}</math> projectile were deduced and compared with those obtained for other strongly bound projectiles, viz., <math>^{12,13}\text{C}</math>, <math>^{16}\text{O}</math>, and <math>^{19}\text{F}</math>, in order to get some systematics in fusion reactions. The analysis of experimental fusion functions was performed within the framework of a benchmark curve called the universal fusion function (UFF). A suppression of about 5–25% with respect to UFF was observed for the presently studied systems at energies above the Coulomb barrier, indicating that the suppression is essentially due to the prompt breakup of the projectiles and is a strong function of breakup threshold of projectiles. The magnitude of such suppression was found to be lower for <math>^{14}\text{N}</math> projectile as compared to other strongly bound projectiles. Moreover, an interesting exponential relation between the experimentally deduced suppression factor and the breakup threshold of the projectile was obtained.</p>
66.	<p><a href="#">The IEEE EPS Packaging Benchmark Suite</a>  F Guo, K Aygün, WD Becker, SG Talocia...R Sharma... - IEEE 30th Conference on Electrical Performance of Electronic Packaging and Systems, 2021</p> <p><b>Abstract:</b> The current state of the Packaging Benchmark Suite being developed by the IEEE EPS technical committee on electrical design, modeling, and simulation (TC-EDMS) is reviewed. The history and goals of the effort to establish the Suite, the key requirements from benchmarks that can support advances in simulation tools and computational methods, and the process being followed by the volunteer committee formed by the authors to produce the Suite are described. The first three benchmarks in the Suite and the steps that were taken to elevate them from potential candidates to effective benchmarks are presented.</p>
67.	<p><a href="#">The SARS-CoV-2 mutation versus vaccine effectiveness: new opportunities to new challenges</a>  JA Malik, S Ahmed, A Mir, M Shinde, O Bender... - Journal of Infection and Public Health, 2022</p> <p><b>Abstract:</b>  Background  The SARS-CoV-2 coronavirus epidemic is hastening the discovery of the most efficient vaccines. The development of cost-effective vaccines seems to be the only solution to terminate this pandemic. However, the vaccines' effectiveness has been questioned due to recurrent mutations in the SARS-CoV-2 genome. Most of the mutations are associated with the spike protein, a vital target for several marketed vaccines. Many countries were highly affected by the 2nd wave of the SARS-CoV-2, like the UK, India, Brazil and France. Experts are also alarming the further COVID-19 wave with the emergence of Omicron, which is highly affecting the South African populations. This review encompasses the detailed description of all vaccine candidates and COVID-19 mutants that will add value to design further studies to combat the COVID-19 pandemic.</p> <p>Methods  The information was generated using various search engines like google scholar, PubMed, clinicaltrial.gov.in, WHO database, ScienceDirect, and news portals by using keywords SARS-CoV-2 mutants, COVID-19 vaccines, efficacy of SARS-CoV-2 vaccines, COVID-19 waves.</p>

	<p><b>Results</b> This review has highlighted the evolution of SARS-CoV-2 variants and the vaccine efficacy. Currently, various vaccine candidates are undergoing several phases of development. Their efficacy still needs to check for newly emerged variants. We have focused on the evolution, multiple mutants, waves of the SARS-CoV-2, and different marketed vaccines undergoing various clinical trials and the design of the trials to determine vaccine efficacy.</p> <p><b>Conclusion</b> Various mutants of SARS-CoV-2 arrived, mainly concerned with the spike protein, a key component to design the vaccine candidates. Various vaccines are undergoing clinical trial and show impressive results, but their efficacy still needs to be checked in different SARS-CoV-2 mutants. We discussed all mutants of SARS-CoV-2 and the vaccine's efficacy against them. The safety concern of these vaccines is also discussed. It is important to understand how coronavirus gets mutated to design better new vaccines, providing long-term protection and neutralizing broad mutant variants. A proper study approach also needs to be considered while designing the vaccine efficacy trials, which further improved the study outcomes. Taking preventive measures to protect from the virus is also equally important, like vaccine development.</p>
68.	<p><a href="#">Topological phase transition associated with structural phase transition in ternary half Heusler compound LiAuBi</a> A Yadav, S Kumar, M Muruganathan, R Kumar - Journal of Physics: Condensed Matter, 2022</p> <p><b>Abstract:</b> In this article, we report detailed theoretical investigations of topological phases in a new non-centrosymmetric half Heusler compound LiAuBi upto a pressure of 30 GPa. It is found that the compound forms into a dynamically stable face centered cubic (FCC) lattice structure of space group <math>Fm\bar{3}m</math> (216) at ambient pressure. The compound is topologically non-trivial at ambient pressure, but undergoes a quantum phase transition to trivial topological phase at 23.4 GPa. However, the detailed investigations show a structural phase transition from FCC lattice (space group 216) to a honeycomb lattice (space group 194) at 13 GPa, which is also associated with a non-trivial to trivial topological phase transition. Further investigations show that the compound also carries appreciable thermoelectric properties at ambient pressure. The figure of merit (ZT) increases from 0.21 at room temperature to a maximum value of 0.22 at 500K. The theoretical findings show its potential for practical applications in spintronics as well as thermoelectricity, therefore LiAuBi needs to be synthesized and investigated experimentally for its applications.</p>
69.	<p><a href="#">Towards the Development of a Task Oriented Robotic Assistance in Vertical Farming</a> R Kumar - Advances in Robotics-5th International Conference of The Robotics Society, 2021</p> <p><b>Abstract:</b> This paper focuses at the planning of a robotic assistive system in a modular vertical farm facility. Smart vertical farms are designed particularly for indoor systems with artificial environment control covering a small area of land but utilizing dimensions through vertical height. A layout of a proposed vertical farm is presented with a 4-Degrees of Freedom (DoF) robotic manipulator to cover three major tasks. The Task Space Locations (TSLs) are identified based upon the transplantation of the seedlings from the seedling tray into the pots of the hydroponic system. The prescribed tasks are simulated for a 4-DoF Kinova manipulator within the design vertical farm environment using Robot Operating System (ROS). It is also planned to develop a work cell for experimental validation of the planned assistance.</p>

[WheatNet-Lite: A Novel Light Weight Network for Wheat Head Detection](#)

S Bhagat, M Kokare, V Haswani, P Hambarde... - Proceedings of the IEEE/CVF International Conference on Computer Vision Workshops, 2021

70. **Abstract:** Recently, the potential for wheat head detection has been significantly enhanced using deep learning techniques. However, the significant challenges are variation in growth stages of wheat heads, canopy, genotype, and wheat head orientation. Furthermore, the wheat head detection task gets even more complex due to the overlapping density of wheat heads and the blur image due to the wind. For real-time wheat head detection, designing lightweight deep learning models for edge devices is also challenging. This paper proposes a lightweight WheatNet-Lite architecture to enhance the efficiency and accuracy of wheat head detection. The proposed method utilizes Mixed Depthwise Conv (MDWConv) with an inverted residual bottleneck in the backbone. Additionally, the Modified Spatial Pyramidal Polling (MSPP) effectively extracts the multi-scale features. The final wheat head bounding box prediction is achieved using WheatNet-lite Neck by utilizing Depthwise Convolution (DWConv) with a Feature Pyramid structure. It reduces 54.2 M network parameters in comparison to YOLOV3. The proposed approach outperforms the existing state-of-the-art methods with mean average precision (mAP) of 91.32 mAP@0.5 and 86.10 mAP@0.5 on GWHD and SPIKE datasets, respectively, with only 8.2 M parameters. Also, the new ACID dataset is proposed with bounding box annotation with 76.32 mAP@0.5. The experimental results are demonstrated on three different datasets viz. Global Wheat Head Detection (GWHD), SPIKE dataset, and Annotated Crop Image Dataset (ACID) showing a significant improvement in the wheat head detection with speed and accuracy.

**Disclaimer:** This publication digest may not contain all the papers published. Library has compiled the publication data as per the alerts received from Scopus and Google Scholar for the affiliation “Indian Institute of Technology Ropar” for the month of January 2022. The author(s) are requested to share their missing paper(s) details if any, for the inclusion in the next publication digest.